Modulation of Atlantic aerosols by the Madden-Julian Oscillation

Baijun Tian,[1] Duane E. Waliser,[1] Ralph A. Kahn,[2] and Sun Wong[1]

Received 17 October 2010; revised 3 June 2011; accepted 9 June 2011; published 10 August 2011.

[1] Our previous study found large intraseasonal variations in satellite-derived aerosol products over the tropical Atlantic Ocean associated with the Madden-Julian Oscillation (MJO). This study aims to investigate the physical mechanism of these aerosol anomalies through analyzing aerosol optical thickness (AOT) from the Moderate Resolution Imaging Spectroradiometer (MODIS) instrument on board the Aqua satellite, precipitation from the Tropical Rainfall Measuring Mission (TRMM) satellite, and low-level (averaged from 925 hPa to 700 hPa) horizontal winds from the National Centers for Environmental Prediction/National Center for Atmospheric Research (NCEP/NCAR) reanalysis. We first show that the intraseasonal variance related to the MJO accounts for about 25% of the total variance of MODIS AOT over the tropical Atlantic. Thus, the intraseasonal variability is one of the important forms of Atlantic aerosol variability. Second, although still inconclusive, our research indicates that precipitation anomalies may play a small role in AOT anomalies through the wet scavenging effect. Third, we show that the AOT anomalies are negatively correlated with the low-level zonal wind anomalies over most parts of the tropical Atlantic, especially over the equatorial Atlantic (60°W–10°W, 10°S–15°N), when the low-level zonal wind anomalies lead the AOT anomalies by about one MJO phase (6 days). When enhanced MJO convection is located over the equatorial Indian Ocean (western Pacific), persistent low-level westerly (easterly) anomalies over the equatorial Atlantic suppress (enhance) the background trade winds that cause the negative (positive) AOT anomalies over the Atlantic region. These results indicate that the AOT anomalies over the tropical Atlantic are very likely produced by the low-level zonal wind anomalies there, although the detailed mechanisms are still to be determined. This study implies that Atlantic aerosol concentration might have predictable components with lead times of 2–4 weeks given the predictability of the MJO and Atlantic trade winds.

Citation: Tian, B., D. E. Waliser, R. A. Kahn, and S. Wong (2011), Modulation of Atlantic aerosols by the Madden-Julian Oscillation, *J. Geophys. Res.*, *116*, D15108, doi:10.1029/2010JD015201.

1. Introduction

[2] The Madden-Julian Oscillation (MJO) [*Madden and Julian*, 1971, 1972] is the dominant form of the intraseasonal (30–90 day) variability in the tropical atmosphere and is characterized by slow (~5 m s^{-1}) eastward-propagating, large-scale oscillations in the tropical deep convection and baroclinic winds, especially over the warmest tropical waters in the equatorial Indian Ocean and western Pacific, during boreal winter (November–April), when the Indo-Pacific warm pool is centered near the equator [*Lau and Waliser*, 2005; *Zhang*, 2005]. It has been well documented that the MJO can impact numerous physical weather and climate phenomena over the globe. However, the impact of the MJO on atmospheric composition is only beginning to be realized [e.g., *Li et al.*, 2010; *Tian et al.*, 2007, 2008; *Weare*, 2010; *Wong and Dessler*, 2007].

[3] Recently, *Tian et al.* [2008] examined the aerosol variability related to the MJO using multiple, global satellite aerosol products including aerosol index (AI) from the Total Ozone Mapping Spectrometer (TOMS) on Nimbus 7 satellite and aerosol optical thickness (AOT) from the Moderate Resolution Imaging Spectroradiometer (MODIS) on Terra satellite and the Advanced Very High Resolution Radiometer (AVHRR) on NOAA satellites. That analysis indicated large intraseasonal variations in the satellite-derived aerosol products over the whole Tropics [*Tian et al.*, 2008, Figures 2 and 4]. Over the tropical Indian Ocean and western Pacific where MJO convection is active and the background aerosol level is low, a strong inverse linear relationship between the TOMS AI and precipitation anomalies, but a weaker, less coherent positive correlation between the MODIS/AVHRR AOT and precipitation anomalies, were found. Although a number of plausible mechanisms for these relationships exist, the exact causes are still to be determined. However, the cloud contamination

[1]Jet Propulsion Laboratory, California Institute of Technology, Pasadena, California, USA.
[2]NASA Goddard Space Flight Center, Greenbelt, Maryland, USA.

Copyright 2011 by the American Geophysical Union.
0148-0227/11/2010JD015201

effect seems to play an important role for the observed relationship [*Tian et al.*, 2008].

[4] Over the equatorial Atlantic Ocean and Africa where MJO convection is weak but the background aerosol level is high, the spatial and temporal patterns of TOMS AI and MODIS AOT anomalies are similar. When the enhanced MJO convection is located over the equatorial Indian Ocean (western Pacific), the aerosol anomalies over the equatorial Atlantic Ocean and Africa are negative (positive). Since the MJO convection and associated cloud anomalies are rather weak over the equatorial Atlantic Ocean and Africa, the cloud contamination effect for the AOT MJO anomalies should be weak too over this region [*Tian et al.*, 2008]. However, how the MJO generates these aerosol variations over the equatorial Atlantic Ocean and Africa was not addressed in *Tian et al.* [2008]. The purpose of the present study is to investigate how the MJO generates these intraseasonal aerosol variations over the equatorial Atlantic Ocean and modulates the Atlantic aerosol concentration.

[5] Many previous studies have suggested that the MJO can have a remote influence on the African and Atlantic region and can modulate precipitation, low-level winds, and African easterly wave activity there [*Foltz and McPhaden*, 2004; *Maloney and Shaman*, 2008; *Matthews*, 2004]. For example, *Foltz and McPhaden* [2004] first found a significant modulation of Atlantic trade winds by the MJO. *Matthews* [2004] documented 20–200 day variability in low-level winds and convection over the eastern Atlantic and sub-Saharan Africa during boreal summer, and he suggested a connection to the global MJO. *Maloney and Shaman* [2008] further studied the intraseasonal variability of boreal summer precipitation and winds in tropical West Africa and the east Atlantic and their results support the important role of the MJO in Atlantic low-level wind variability as suggested by Matthews. The purpose of the present study is to investigate whether the MJO can modulate the intraseasonal aerosol variations over the equatorial Atlantic Ocean through its influence on Atlantic precipitation and low-level wind.

[6] Given the potential predictability of the MJO extending to 2–4 weeks [e.g., *Waliser*, 2005], if the MJO does influence the Atlantic aerosols, then the Atlantic aerosol concentration may be predictable with lead times of 2–4 weeks, which in turn may lend important guidance to prediction of air quality, dust storm activity, and ocean nutrient deposition over the Atlantic Ocean. Furthermore, the modulation of Atlantic aerosols by the MJO will provide an important physical-chemical process to evaluate chemical transport models and help model development.

[7] Sections 2 and 3 describe the data sets and MJO analysis methodology used in this study. Section 4 presents the MJO-related Atlantic AOT anomalies from MODIS/Aqua and a comparison to those from MODIS/Terra. Sections 5 and 6 show the role of MJO-related precipitation and low-level zonal wind anomalies in the Atlantic AOT anomalies, followed by a discussion in section 7. Conclusions of this paper are summarized in section 8.

2. Data

[8] For this study, we use the MODIS/Aqua Collection 5.1 (C051), Level-3 (L3) daily global aerosol product Optical_Depth_Land_and_Ocean_Mean (MYD08 D3). The data are on 1° × 1° spatial grids and cover the period from 4 July 2002 to 1 June 2009. This aerosol product represents total-column AOT at 0.55 μm for each 1° × 1° spatial grid over both ocean (best) and land (corrected) except for bright surfaces based on the dark target algorithm [*Kaufman et al.*, 1997; *Levy et al.*, 2007a, 2007b; *Remer et al.*, 2008; *Tanré et al.*, 1997]. It is derived from the MYD04 L2 (10 × 10 1 km pixel array) Scientific Data Set (SDS) Optical_Depth_Land_and_Ocean_Mean using the simple numerical average with the quality assurance confidence (QAC) flag ≥1 over ocean and QAC flag = 3 over land. Note that the land part of this SDS is taken from the MYD04 L2 SDS Corrected_Optical_Depth_Land_Mean at 0.55 μm, and the ocean part of this SDS is taken from the MYD04 L2 SDS Effective_Optical_Depth_Best_Ocean_Mean [*Levy et al.*, 2009]. The expected error for this MODIS aerosol product is that 1 standard deviation of AOT retrievals would fall within ± (0.03 + 0.05 AOT) over ocean and ± (0.05 + 0.15 AOT) over land. Validation studies indicate that over ocean, the MODIS AOT retrievals were within the expected error bounds. Over land, in some cases the MODIS AOT retrievals fell within expected uncertainties, but in many situations there appeared to be a strong positive bias at low AOT retrievals and a negative bias at high AOT retrievals [e.g., *Levy et al.*, 2010; *Remer et al.*, 2008]. Furthermore, the misidentified cloudy pixels can further induce uncertainties for the MODIS AOT retrievals [e.g., *Kaufman et al.*, 2005b; *Tian et al.*, 2008].

[9] To identify the potential role of precipitation in the AOT anomalies, we use the Tropical Rainfall Measurement Mission (TRMM) 3B42 Version 6 precipitation data from 1 January 1998 to 30 June 2009. The TRMM 3B42 data extends globally from 50°S–50°N on 0.25° × 0.25° grid boxes every 3 h [*Huffman et al.*, 2007]. For this work, the precipitation data are averaged daily on 1° × 1° spatial grids. To characterize the large-scale circulation patterns that transport aerosols, data for daily horizontal winds from the National Centers for Environmental Prediction/National Center for Atmospheric Research (NCEP/NCAR) reanalysis are used. The wind data have a spatial resolution of 2.5° × 2.5° and cover the period 2002–2009. Since aerosols are mainly located in the lower troposphere (below 600 hPa) [*Chiapello et al.*, 1995; *Huang et al.*, 2010], we use the low-level horizontal winds averaged from 925 hPa to 700 hPa for our analysis.

[10] To demonstrate the regional variations of the reliability of the MODIS AOT retrievals, Figure 1a shows the climatological mean (2002–2009) boreal winter percentage of valid data points (pixels) within each 1° × 1° spatial grid for MODIS/Aqua C051 L3 AOT data (colored areas) over the tropical Atlantic region (70°W–30°E, 20°S–30°N). It is calculated by dividing the value of the SDS Optical_Depth_Land_and_Ocean_Pixel_Counts by the total pixel counts within each 1° × 1° spatial grid. That latter is calculated by dividing the area of that grid by the each pixel area (100 km^2). To highlight the role of convective clouds in the spatial distribution of the percentage of the valid data points, the climatological mean (2002–2009) TRMM precipitation is also shown in black contours in Figure 1a. Figure 1a indicates that the percentage of valid data points within each 1° × 1° spatial grid for the MODIS AOT data range

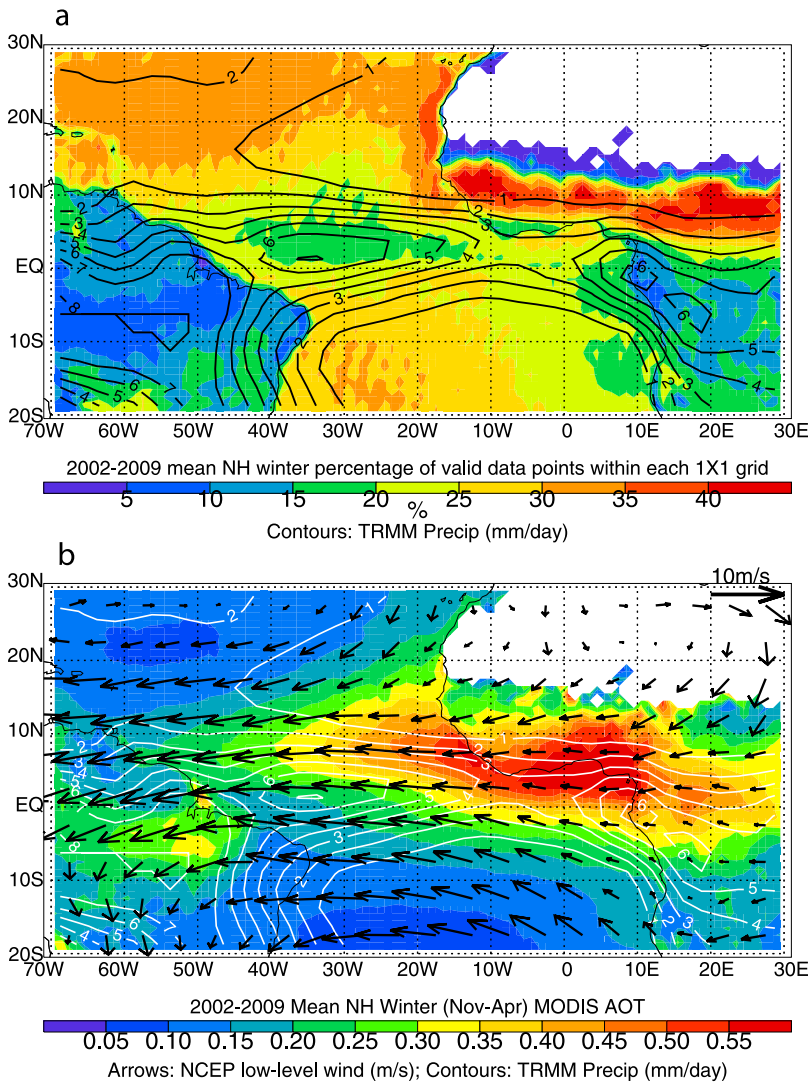

Figure 1. (a) Climatological mean (2002–2009) boreal winter (November–April) percentage of valid data points within each 1° × 1° spatial grid for the Moderate Resolution Imaging Spectroradiometer (MODIS)/Aqua C051 L3 aerosol optical thickness (AOT) data (colored areas) and the Tropical Rainfall Measuring Mission (TRMM) precipitation (mm day^{-1}) (black contours) over the tropical Atlantic region. White areas indicate missing MODIS AOT data. (b) Climatological mean (2002–2009) boreal winter MODIS AOT (colored areas), TRMM precipitation (mm day^{-1}) (white contours) and National Centers for Environmental Prediction/National Center for Atmospheric Research (NCEP/NCAR) low-level (averaged from 925 to 700 hPa) horizontal winds (arrows) over the tropical Atlantic region.

from 0% to ~40% depending on the regional surface and atmospheric conditions. For example, there are no valid data at all (0%) over the Saharan Desert because of bright surfaces there. Very low values (≤20%) are located in the tropical deep convective regions, the so-called Intertropical Convergence Zone (ITCZ), such as equatorial South America, equatorial South Africa, and equatorial Atlantic, where deep convective clouds and heavy precipitation (>4 mm day^{-1}) are prevalent and clear-sky pixels are rare there. Relative high values (>30%) are generally found in the clear subsiding subtropics, such as subtropical North and South Atlantic. There is a clear land-sea contrast in the percentage of valid data points. In general, it is much lower over land than over oceans because of the complex land surface conditions. However, it is much higher (~45%) over the Sahel region with dark lands (vegetation and soils), where the MODIS dark target aerosol algorithm works well. All the missing values in bright surfaces or deep convective regions were neglected in our analysis, without any filling using the neighboring values.

[11] Figure 1b shows the climatological mean (2002–2009) boreal winter MODIS AOT (colored areas), TRMM precipitation (white contours) and NCEP/NCAR low-level horizontal winds (arrows) over the tropical Atlantic region. In Figure 1b, the strong impact of land surface aerosol emission and large-scale low-level horizontal, especially zonal, wind aerosol transport is evident in the aerosol distribution. For example, large aerosol loadings are found near the Sahara desert due to strong sources of desert dust and over equatorial Africa and Amazon associated with biomass

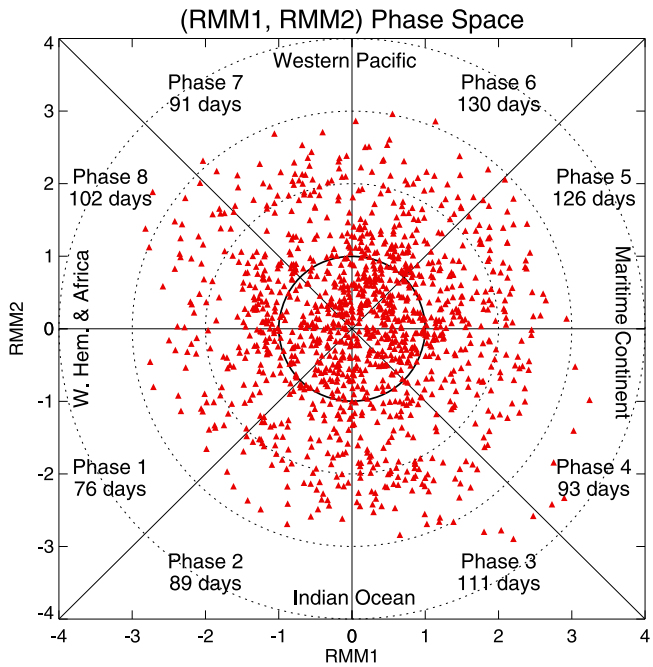

Figure 2. RMM1 and RMM2 phase space for all days in boreal winter from November 2002 to April 2009 and the number of days for each phase of the Madden-Julian Oscillation (MJO) cycle. Eight defined phases of the phase space are labeled to indicate the eastward propagation of the MJO in one MJO cycle. Also labeled are the approximate locations of the enhanced convective signal of the MJO for that location of the phase space, e.g., the Indian Ocean for phases 2 and 3.

burning activities [*Kaufman et al.*, 2005a]. The dominant aerosol feature over the tropical Atlantic is the zonally oriented optically thick aerosol plume centered at 5°N–8°N stretching across the Atlantic. Its magnitude (>0.6) and latitudinal extent (~15°S–20°N) are greatest over the eastern equatorial Atlantic along the west coast of Africa and gradually decrease westward toward the central and western equatorial Atlantic. It can reach the northeast coast of South America and Amazon basin with sizable AOT values (~0.2). This aerosol plume is the result of the equatorial Atlantic trade winds that transport the mixed Saharan/Sahelian dust and biomass-burning smoke from Africa to the Atlantic Ocean [e.g., *Cakmur et al.*, 2001; *Carlson and Prospero*, 1972; *Huang et al.*, 2010; *Husar et al.*, 1997; *Kaufman et al.*, 2005a]. Over the subtropical North and South Atlantic (~25°N/S), two high-pressure anticyclones (e.g., Azores high) dominate, and the aerosol loading there is very low (~0.05). It is also noted that the Atlantic aerosol plume is mainly located at the northern edge of the ITCZ. This indicates that precipitation may play some role in the aerosol distribution but not as important a role as the low-level wind aerosol transport.

3. Analysis Methodology

[12] For the MJO analysis and composite procedure, we use the multivariate empirical orthogonal function (EOF) method introduced by *Wheeler and Hendon* [2004] and adopted widely by the MJO community [e.g., *Waliser et al.*, 2009]. The comparison of this multivariate EOF method and the extended EOF method used in our previous aerosol study [*Tian et al.*, 2008] has been examined by *Tian et al.* [2010] with the finding that both methods yield similar results for the MJO composite analysis. Briefly, the intraseasonal anomalies of daily aerosol and wind data were obtained by removing the climatological mean seasonal cycle and filtering via a 30–90 day band pass filter. Then, a composite MJO cycle (8 phases) was calculated by averaging the daily anomalies that occurred within each phase of the MJO cycle. The MJO phase for each day is determined by the Real-time Multivariate MJO (RMM) index (a pair of PC time series called RMM1 and RMM2, available at http://www.bom.gov.au/climate/mjo/ for 1974 to the present). Figure 2 shows the (RMM1 and RMM2) phase space for all days in boreal winter from November 2002 to April 2009 and the number of days for each phase of the composite MJO cycle. Only days with strong MJO activity ($RMM1^2 + RMM2^2 \geq 1$) are considered. The statistical assessment as to whether a composite mean at each point is different from zero is assessed by the two-sided Student's t test similar to the procedure of *Weare* [2010]. If the absolute value of the composite mean is greater than $t\sigma/\sqrt{N}$, then it is considered to be statistically significant with the specified confidence limit. Here, N is the effective number of the AOT samples, σ is the standard deviation of the AOT samples for each phase of the composite MJO cycle, and t is the t distribution value determined by N and the specified confidence limit. Because the composite means are calculated from data that are highly filtered and thus have substantial autocorrelations, N is smaller than the actual number of the AOT samples for each phase of the composite MJO cycle. In this analysis, the ratio of the effective number of samples relative to the actual number of samples is estimated using the lag correlations of the RMM1 following the procedure described by *Leith* [1973], and it is about 1/11.4.

4. MJO-Related Atlantic AOT Anomalies

[13] Figure 3 shows the composite maps of boreal winter MJO-related MODIS AOT anomalies (multiplied by 100) over the tropical Atlantic region. The contours show all AOT anomalies, while the colored areas show only AOT anomalies above a 90% confidence limit at the intervals of 0.01. Solid contours (red) indicate positive AOT anomalies while dashed contours (blue) indicate negative AOT anomalies. In Figure 3 we see large AOT anomalies over the equatorial Atlantic, collocated with the background aerosol plume (Figure 1b). The highest magnitude (±0.04) and largest latitudinal extent (~15°S–20°N) of these AOT anomalies are typically found over the eastern equatorial Atlantic along the west coast of Africa. The AOT anomalies range up to about ±0.04 for the composite MJO and are about 20% of their background mean (~0.2) (Figure 1b). However, the AOT anomalies for individual MJO events are about ±0.2 and can be as large as ±0.8. These AOT anomalies for individual MJO events are much larger than MODIS AOT uncertainty (±0.03 over ocean and ±0.05 over land) [*Remer et al.*, 2005, 2008] and comparable to the AOT

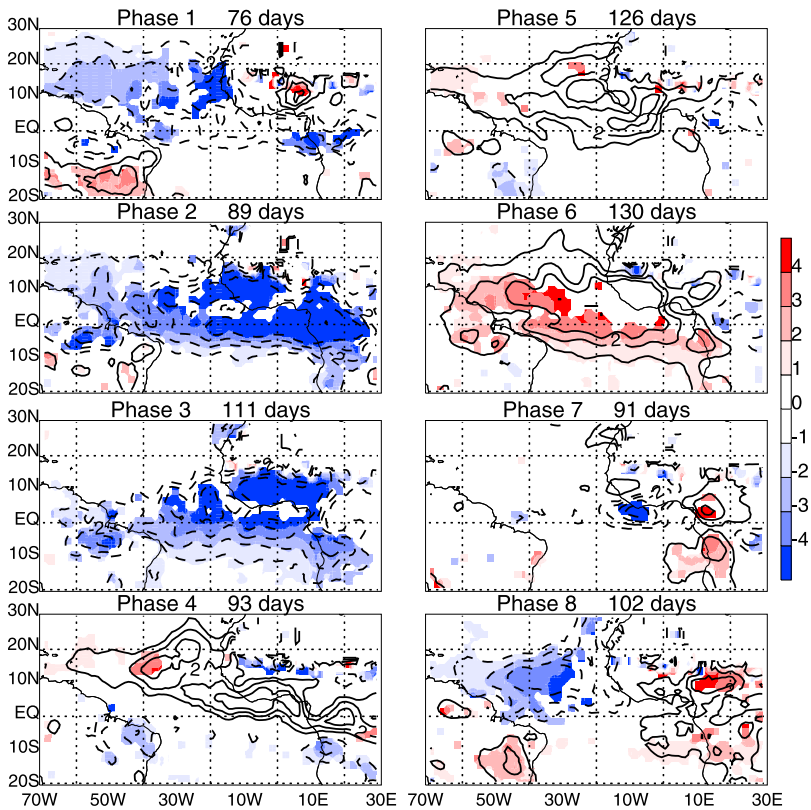

Figure 3. Composite maps of boreal winter MJO-related MODIS AOT anomalies (multiplied by 100) over the tropical Atlantic region. The contours show all AOT anomalies, while the colored areas show only AOT anomalies above a 90% confidence limit at intervals of 0.01. Solid contours (red) indicate positive AOT anomalies, while dashed contours (blue) indicate negative AOT anomalies.

anomalies caused by dust storms at synoptic scale (~0.2) [*Wong et al.*, 2006]. To demonstrate the importance of the intraseasonal variations of the Atlantic aerosols in their overall variability, Figure 4 shows the standard deviations of boreal winter AOT anomalies for all time scales (≥2 days) after removing the climatological mean seasonal cycle (Figure 4a) and those for the intraseasonal time scale after removing the climatological mean seasonal cycle and filtering via a 30–90 day band pass filter (note the color scale change) (Figure 4b) as well as the percentage of the total variance of boreal winter AOT anomalies explained by their intraseasonal variance (Figure 4c). The spatial patterns of the standard deviations of boreal winter AOT anomalies for both all and intraseasonal time scales are similar to that of the mean AOT in Figure 1b. The total standard deviations are about half of the mean AOT values while the intraseasonal standard deviations are about half of the total standard deviations. As a result, the intraseasonal variance accounts for about 25% of the total variance of the aerosol variability over the tropical Atlantic (e.g., 5°S–15°N). Thus, intraseasonal variability is one important form of aerosol variability over the Atlantic region. To further demonstrate the importance of intraseasonal variability, Figure 5 shows the time series spectrum of the unfiltered MODIS AOT anomalies after removing the climatological mean seasonal cycle averaged over the equatorial Atlantic (30°W–15°W, EQ–15°N), where the MODIS AOT anomalies are large. Red lines show the red noise spectrum and its upper 90% confidence limit. Clearly, there is a strong intraseasonal peak (30–60 days) above a 90% confidence limit in the spectrum of Atlantic AOT.

[14] It is also interesting to note that the percentage of AOT variability attributable to intraseasonal variance over the continent is much lower compared to the adjacent ocean region (Figure 4c). The exact reasons for such a land-sea difference are still unknown to us. However, one possible explanation is the retrieval artifact of MODIS AOT data because MODIS uses different aerosol algorithms for land and ocean and there is a clear land-sea contrast in percentage of valid data points within each 1° × 1° spatial grid for the MODIS AOT data (Figure 1a).

[15] For a comparison between the current MODIS/Aqua C051 results and our earlier MODIS/Terra C004 results, the phases 2, 4, 6, and 8 in Figure 3 roughly correspond to the lags 0, +2, +4, and −2 in *Tian et al.* [2008, Figure 4] according to the location of MJO convection (precipitation) anomalies [see *Tian et al.*, 2008, Figure 4; *Waliser et al.*, 2009, Figure 12]. A comparison of Figure 3 and *Tian et al.* [2008, Figure 4] indicates that the general spatial and temporal patterns and magnitudes of AOT anomalies over the Atlantic region are similar between MODIS/Aqua and MODIS/Terra. For example, both phase 2 in Figure 3 and lag 0 in *Tian et al.*

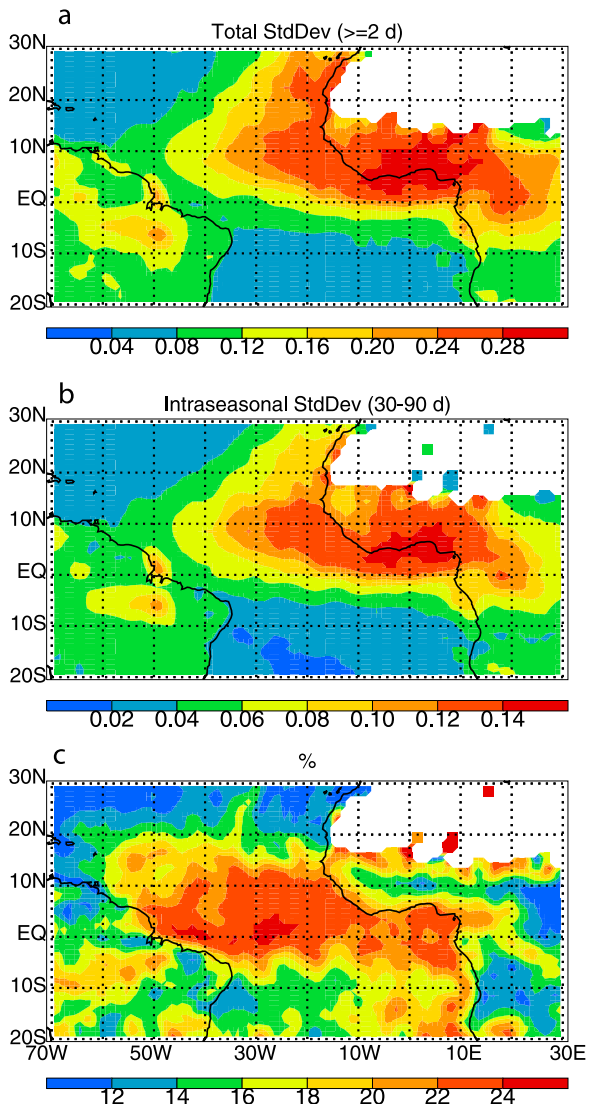

Figure 4. (a) Standard deviation of boreal winter MODIS AOT anomalies for all time scales after removing the mean seasonal cycle (≥2 days, total); (b) Same as (a) except for intraseasonal time scale after removing the mean seasonal cycle and filtering via a 30–90 day band pass filter; (c) Percentage of the total variance of boreal winter MODIS AOT anomalies explained by their intraseasonal variance.

[2008, Figure 4] show strong negative AOT anomalies over the tropical Atlantic when the enhanced convection is located over the central and eastern equatorial Indian Ocean. In contrast, both phase 6 in Figure 3 and lag +4 in *Tian et al.* [2008, Figure 4] show strong positive AOT anomalies over the tropical Atlantic when the enhanced convection is located over the equatorial western Pacific. Furthermore, both phase 4 in Figure 3 and lag +2 in *Tian et al.* [2008, Figure 4] show weak positive AOT anomalies over the tropical North Atlantic and weak negative AOT anomalies over the tropical South Atlantic when the enhanced convection is located over the Maritime Continent, and the converse holds for phase 8 in Figure 3 and lag −2 in *Tian et al.* [2008, Figure 4]. The global spatial and temporal patterns of MODIS/Aqua and MODIS/Terra AOT anomalies are also similar (not shown).

5. Role of MJO-Related Precipitation Anomalies

[16] In this section, we show the potential role of precipitation anomalies associated with the MJO in modulating the intraseasonal Atlantic AOT anomalies. Figure 6 shows the composite maps of boreal winter MJO-related MODIS AOT anomalies (multiplied by 100) and TRMM precipitation anomalies over the tropical Atlantic region. Figure 7 shows their linear lag correlation for the composite MJO cycle. The negative correlation implies the wet scavenging effect of precipitation on aerosols while the positive correlation may indicate the potential cloud contamination effect of MODIS AOT data as discussed in our previous paper [*Tian et al.*, 2008]. Negative lags (e.g., lag −2 or −1) mean precipitation anomalies lead AOT anomalies (by 2 or 1 MJO phases) while positive lags (e.g., lag +1) indicate precipitation anomalies lag AOT anomalies (e.g., by 1 MJO phase). Figure 6 demonstrates precipitation anomalies over Atlantic are rather weak and mainly located in the ITCZ where AOT anomalies are small. Over the North Atlantic where AOT anomalies are large, precipitation anomalies are almost negligible. This indicates that the precipitation anomalies should play a very small role in the AOT anomalies or the precipitation anomalies cannot fully explain the AOT anomalies by themselves alone if the precipitation anomalies play any role at all in the AOT anomalies. Figure 7 indicates that when precipitation anomalies lead AOT anomalies, negative correlation between precipitation anomalies and AOT anomalies is found over some parts of the Atlantic. This indicates that precipitation anomalies may impact AOT anomalies through the wet scavenging effect. However, over some regions, especially the equatorial North Atlantic (10°N–EQ), positive correlation between precipitation and AOT anomalies is found. This positive correlation may be due to the cloud contamination effect of the MODIS AOT data [*Tian et al.*, 2008]. Thus, Figures 6 and 7 indicate that the precipitation anomalies may play a role in the AOT

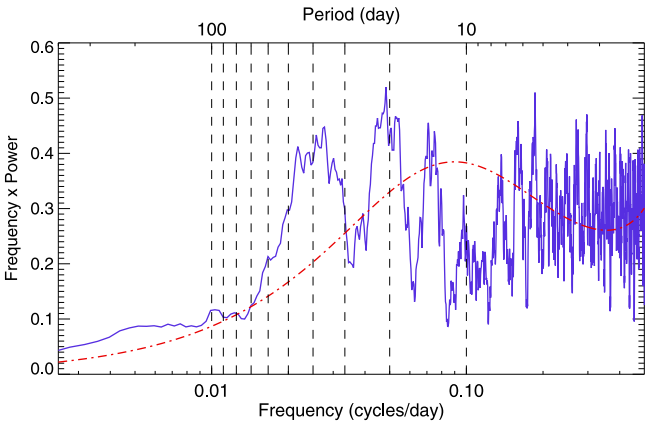

Figure 5. The time series spectrum of the unfiltered MODIS AOT anomalies after removing the annual cycle averaged over the equatorial Atlantic (30°W–15°W, EQ–12°N) where the MODIS AOT anomalies are large. Red line shows the red noise spectrum and its upper 90% confidence limit.

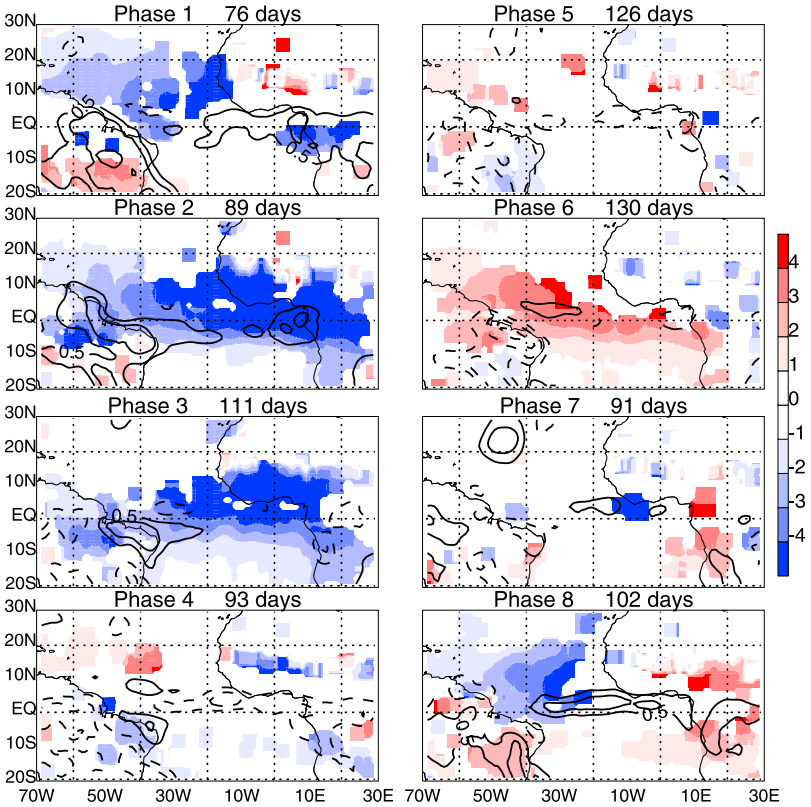

Figure 6. Composite maps of boreal winter MJO-related MODIS AOT anomalies (multiplied by 100) (colored areas) and TRMM 3B42 precipitation anomalies (mm day^{-1}) (contours) over the tropical Atlantic region. Only AOT anomalies above a 90% confidence limit are shown. Solid contours indicate positive precipitation anomalies, while dashed contours indicate negative precipitation anomalies at a 0.5 mm day^{-1} interval.

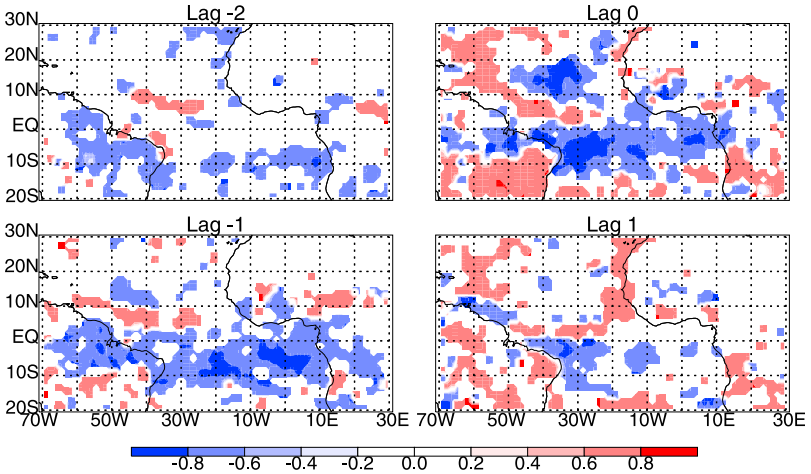

Figure 7. Linear lag correlation coefficient between the boreal winter MJO-related MODIS AOT anomalies and TRMM precipitation anomalies over the tropical Atlantic region. Negative (positive) correlation means that positive precipitation anomalies induce negative (positive) AOT anomalies or negative precipitation anomalies induce positive (negative) AOT anomalies. Negative lags (e.g., lag −2 or −1) mean the precipitation anomalies lead the AOT anomalies (by 2 or 1 MJO phases), while positive lags (e.g., lag +1) indicate the precipitation anomalies lag the AOT anomalies (e.g., by 1 MJO phase). Only correlation coefficients above a 90% confidence limit are shown.

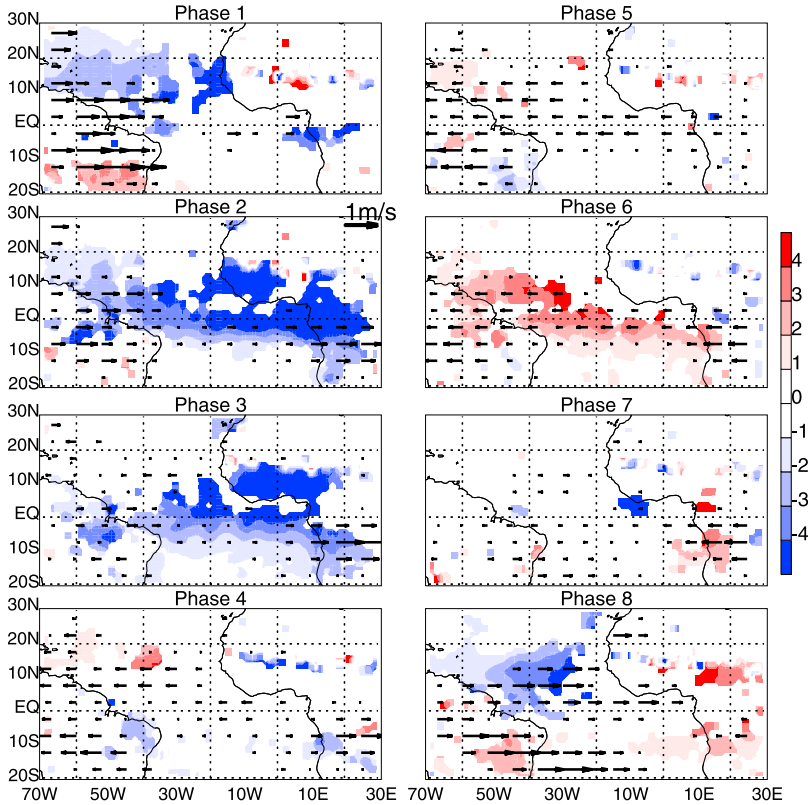

Figure 8. Composite maps of boreal winter MJO-related MODIS AOT anomalies (multiplied by 100) and NCEP/NCAR low-level (averaged from 925 hPa to 700 hPa) zonal wind anomalies (m s^{-1}) over the tropical Atlantic region. Only AOT and wind anomalies above a 90% confidence limit are shown.

anomalies through the wet scavenging effect, but it should be a small one. Furthermore, the cloud contamination effect in the MODIS AOT data has hindered us from reaching a definitive conclusion regarding this issue.

6. Role of MJO-Related Low-Level Zonal Wind Anomalies

[17] In this section, we demonstrate the important role of the low-level trade wind variability associated with the MJO in modulating the intraseasonal Atlantic AOT anomalies. Figure 8 shows the composite maps of boreal winter MJO-related MODIS AOT anomalies (multiplied by 100) and low-level (averaged from 925 hPa to 700 hPa) NCEP/NCAR zonal wind anomalies over the tropical Atlantic region. Figure 8 demonstrates the strong impact of low-level zonal wind anomalies on the Atlantic AOT anomalies. For example, at phase 2, when the enhanced convection is located over the central and eastern equatorial Indian Ocean [*Waliser et al.*, 2009, Figure 12], the low-level zonal wind anomalies over the equatorial Atlantic are persistent westerlies that blow from the Atlantic Ocean (Figure 8) to Africa as a dynamical response to the enhanced convection over the Indian Ocean. These low-level westerly anomalies suppress the background trade winds (reducing the wind speed but not changing the wind direction). As a result, this may reduce the aerosol concentration and cause the negative AOT anomalies over the Atlantic region. A similar argument can also be applied to phases 1 and 3. In contrast, in phase 6, when the enhanced MJO convection is located over the equatorial western Pacific [*Waliser et al.*, 2009, Figure 12], the low-level zonal wind anomalies over the equatorial Atlantic are persistent easterlies that blow from Africa to the Atlantic Ocean (Figure 8) as a dynamical response to suppressed convection over the Indian Ocean. These easterly anomalies enhance the background trade winds (increasing the wind speed but not changing the wind direction) and may cause the positive AOT anomalies over the Atlantic region. Similar reasoning also applies to phases 4 and 5.

[18] To better demonstrate the important role of low-level zonal wind anomalies in the Atlantic AOT anomalies, Figure 9 shows the linear lag correlation between the MODIS AOT anomalies and NCEP/NCAR low-level zonal wind anomalies (Figure 8) for the composite MJO cycle over the tropical Atlantic region. Here, negative (positive) correlation means that westerly anomalies induce negative (positive) AOT anomalies or easterly anomalies induce positive (negative) AOT anomalies. Negative lags (e.g., lag −2 or −1) mean the low-level zonal wind anomalies lead the AOT anomalies (by 2 or 1 MJO phases), while positive lags (e.g., lag +1) indicate the low-level zonal wind anomalies lag the AOT anomalies (e.g., by 1 MJO phase). Figure 9 indicates that the AOT anomalies are negatively correlated with the low-level zonal wind anomalies over most parts of the tropical Atlantic and the west coast of Africa when the low-level zonal wind anomalies lead the AOT anomalies. Over the equatorial Atlantic between 5°S and 12°N where the

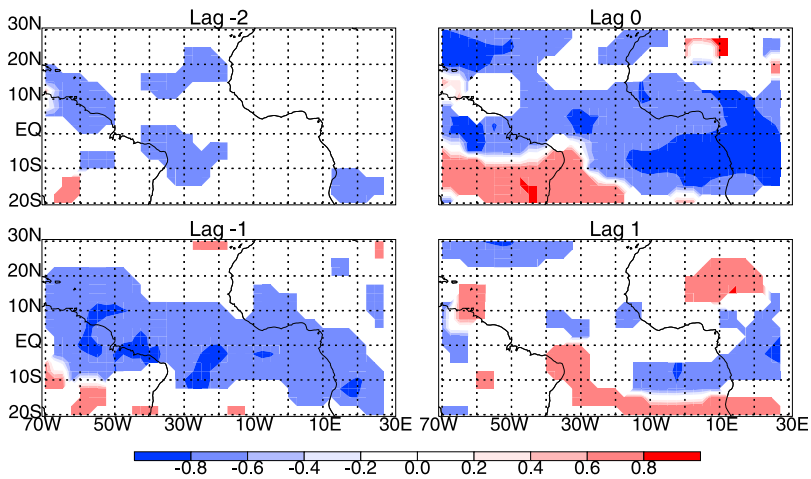

Figure 9. Linear lag correlation coefficient between the boreal winter MJO-related MODIS AOT anomalies and NCEP/NCAR low-level zonal wind anomalies over the tropical Atlantic region. Negative (positive) correlation means that westerly anomalies induce negative (positive) AOT anomalies or easterly anomalies induce positive (negative) AOT anomalies. Negative lags (e.g., lag −2 or −1) mean that the low-level zonal wind anomalies lead the AOT anomalies (by 2 or 1 MJO phases), while positive lags (e.g., lag +1) indicate that the low-level zonal wind anomalies lag the AOT anomalies (e.g., by 1 MJO phase). Only correlation coefficients above a 90% confidence limit are shown.

AOT anomalies are large, the negative correlation appears to peak when the low-level zonal wind anomalies lead the AOT anomalies by about one MJO phase. However, the correlation becomes positive when the low-level zonal wind anomalies lag the AOT anomalies. These results indicate that the AOT anomalies over the Atlantic are very likely produced by the low-level zonal wind anomalies there. In other words, the MJO may modulate the Atlantic aerosols through its influence on the Atlantic low-level zonal wind anomalies.

[19] To further demonstrate this point, Figure 10 shows the composite MJO cycle of MODIS AOT anomalies (solid lines) and NCEP/NCAR low-level zonal wind anomalies (dashed lines) averaged over the equatorial Atlantic (30°W–15°W, EQ–12°N) where the AOT anomalies are large. Figure 10 clearly shows that the MJO cycle of the low-level zonal wind anomalies and AOT anomalies are negatively correlated and that the former lead the latter by about one MJO phase (about 6 days). This result further demonstrates the important role of the low-level zonal wind anomalies for the AOT anomalies over this region.

[20] It is also interesting to note a positive correlation between AOT and zonal wind anomalies over the east coast of South America around (15°S, 40°W), where the background trade winds blow the clean marine air from the south Atlantic to South America (Figure 1b). Thus, westerly (easterly) anomalies may reduce (enhance) the marine air input to the land and enhance (suppress) the local biomass burning activity and aerosol loading.

7. Discussion

[21] It is well known that the Atlantic aerosol concentrations are mainly determined by three factors: aerosol emission over the Africa, westward aerosol transport by the trade winds, and aerosol deposition. Thus, there are three possible ways for the weaker (stronger) trade winds due to the MJO-related westerly (easterly) anomalies to induce the negative (positive) AOT anomalies over the Atlantic region. First, the weaker (stronger) trade winds over the West Africa, commonly referred to the Harmattan [*Bou Karam et al.*, 2008], can reduce (enhance) the aerosol emission over the African continents and aerosol source for the westward transport to the Atlantic Ocean. Second, the weaker (stronger) trade winds over the Atlantic and African coast can reduce (enhance) the westward aerosol transport to the Atlantic Ocean. Third, the weaker (stronger) trade winds over the Atlantic Ocean may enhance (reduce) the aerosol deposition over the Ocean.

[22] Among them, the second mechanism may play an important role for the negative correlation between the low-level zonal wind and AOT anomalies presented in section 6.

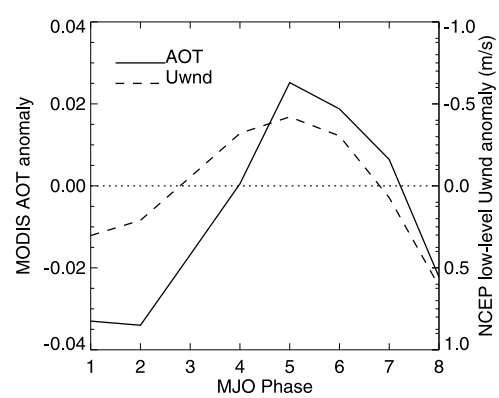

Figure 10. The composite MJO cycle of MODIS AOT anomalies (solid line) and NCEP/NCAR low-level zonal wind anomalies (dashed line) averaged over the equatorial Atlantic (30°W–15°W, EQ–15°N) where the MODIS AOT anomalies are strong.

This speculation is supported by a clear phase lag of about 6 days between the zonal wind anomalies and AOT anomalies which is consistent with the dust transport time scale from Africa to the Atlantic documented in earlier studies [e.g., *Prospero and Carlson*, 1981]. Furthermore, if we assume the aerosol emission and dry deposition do not change at all, and only the weaker (stronger) trade winds caused by westerly (easterly) anomalies weaken (enhance) the total westward aerosol transport, then we should expect the negative (positive) AOT anomalies over the Atlantic Ocean and positive (negative) AOT anomalies over the upstream source regions over the Africa continent. Our results do indicate the contrasting AOT anomalies between the Atlantic Ocean and the upstream African continent. For example, at phase 1, Figure 3 shows negative AOT anomalies over the Atlantic Ocean and positive AOT anomalies over the African continent around 5°E and 10°N. Thus, it is very likely the change of westward aerosol transport due to the trade wind anomalies alone can explain the AOT anomalies over the Atlantic.

[23] However, this study is based mainly on the correlation of spatiotemporal variability of zonal wind and AOT anomalies. It should be noted that atmospheric circulations in the Atlantic region exhibit strong variability on a wide range of space and time scales. This implies some limitations may exist for such analyses relying on the correlation alone. Thus, the relative contribution of changes in aerosol emission, westward aerosol transport, and aerosol deposition due to the trade wind anomalies to the AOT anomalies cannot be fully determined by our current results and needs further investigations in the future based complex chemistry transport models.

[24] Please note that over the South African coast between 10°S and equator (10°S–EQ, 0°–30°E), the largest negative correlations reach maximum when the NCEP/NCAR low-level zonal wind anomalies and MODIS AOT anomalies are in the same MJO phase. This is different from the equatorial Atlantic discussed above. This difference may be due to the different roles of low-level zonal winds in the aerosol distribution between these two regions. The low-level zonal wind anomalies may influence the AOT anomalies through the westward aerosol transport over the equatorial Atlantic but through aerosol emission over the South African coast. This difference may also be a retrieval artifact attributable to large uncertainties of the MODIS AOT data over the South African coast, as evidenced by the very low percentage of valid points over this region in Figure 1a. However, the exact reasons need to be investigated further in the future.

[25] However, there are other caveats for this study. First, because of the cloud contamination effect in the satellite AOT products, the role of precipitation anomalies in the AOT anomalies cannot be fully determined by the satellite data analysis alone. Further future investigations based on complex chemistry transport models are definitely needed. Second, it has been documented that African easterly waves can be efficient mechanisms of transporting African dust westward [*Jones et al.*, 2004; *Karyampudi et al.*, 1999; *Prospero and Carlson*, 1972]. It is also documented that the MJO can modulate the African easterly wave activity over the tropical Atlantic Ocean [e.g., *Matthews*, 2004]. Thus, the AOT anomalies over the Atlantic Ocean may be a result of the changes of westward aerosol transport by the African easterly waves associated with the MJO. This potential mechanism also needs to be further explored in the future.

8. Conclusions

[26] This study aims to investigate the physical mechanism of large intraseasonal variations in tropical Atlantic aerosols found in our previous study [*Tian et al.*, 2008] through analyzing the MODIS/Aqua C051 AOT, TRMM precipitation and NCEP/NCAR low-level horizontal winds. First, through reference to our earlier study, we show that the general spatial and temporal patterns and magnitudes of AOT anomalies over the Atlantic region are similar between MODIS/Aqua C051 and MODIS/Terra C004 data. The intraseasonal variance related to the MJO accounts for about 25% of the total variance of MODIS AOT over the tropical Atlantic. Thus, the intraseasonal variability is one important form of Atlantic aerosol variability.

[27] Second, we have shown that a negative correlation between precipitation anomalies and AOT anomalies is found over some parts of Atlantic. This indicates that precipitation anomalies may impact AOT anomalies through the wet scavenging effect. However, different spatial patterns of precipitation and AOT anomalies indicate that the precipitation anomalies would play a small role in the AOT anomalies. Furthermore, due to the cloud contamination effect in the satellite AOT products, the role of precipitation anomalies in the AOT anomalies cannot be fully determined by the satellite data analysis alone as done in this study.

[28] Third, we show that the AOT anomalies are negatively correlated with the low-level zonal wind anomalies over most parts of tropical Atlantic when the low-level zonal wind anomalies lead the AOT anomalies. Furthermore, we found that the highest negative correlation between the low-level zonal wind anomalies and the AOT anomalies over the equatorial Atlantic (60°W–10°W, 10°S–15°N) occurs when the former lead the latter by about one MJO phase (6 days). When enhanced MJO convection is located over the equatorial Indian Ocean, persistent low-level westerly anomalies over the equatorial Atlantic suppress the background trade winds that cause the negative AOT anomalies over the Atlantic region. In contrast, when enhanced MJO convection is located over the equatorial western Pacific, persistent low-level easterly anomalies over the equatorial Atlantic enhance the background trade winds that cause the positive AOT anomalies over the Atlantic region. These results indicate that the AOT anomalies over the tropical Atlantic are very likely produced by the low-level zonal wind anomalies there. In other words, the MJO may modulate the Atlantic aerosols through its influence on the Atlantic low-level zonal wind anomalies. The low-level zonal wind anomalies can induce the AOT anomalies over the tropical Atlantic through their influences on the following three possible ways: aerosol emission over the African continent, the westward aerosol transport and aerosol deposition over the Atlantic Ocean. It is very likely that the change of the westward aerosol transport due to the low-level zonal wind anomalies plays an important role in the AOT anomalies over the Atlantic Ocean. However, the relative contribution of changes in aerosol emission, westward aerosol transport, and aerosol deposition due to the

trade wind anomalies to the AOT anomalies cannot be fully determined by our current results and requires further investigations in the future based on complex chemistry transport models.

[29] Given the potential predictability of the MJO and Atlantic trade winds extending to 2–4 weeks [e.g., *Foltz and McPhaden*, 2004; *Maloney and Shaman*, 2008; *Matthews*, 2004; *Waliser*, 2005], this study implies that components of the Atlantic aerosol concentration may be predictable with lead times of 2–4 weeks, which in turn may lend important guidance to the climate processes, such as air quality, dust storm, and ocean nutrients, over the Atlantic Ocean. Furthermore, this study provides an important physical-chemical process that can be used to evaluate chemical transport models and to advance model development.

[30] **Acknowledgments.** This research was performed at Jet Propulsion Laboratory (JPL), California Institute of Technology, under a contract with NASA. It was supported in part by the Atmospheric Infrared Sounder (AIRS) project at JPL and National Science Foundation (NSF) grant ATM-0840755 at the University of California, Los Angeles. Comments from three anonymous reviewers, discussions with Lorraine Remer and Robert Levy on the MODIS AOT data, help from Bryan Weare on the statistical significance test, and help from Xun Jiang on the spectrum analysis are gratefully acknowledged. The first author would like to dedicate this paper to his father, HongFang Tian, who passed away in March 2011. Without his father's support and encouragement, there would have been no way for B.T. to grow up in a poor rural village in China and become a scientist in the USA.

References

Bou Karam, D., C. Flamant, P. Knippertz, O. Reitebuch, J. Pelon, M. Chong, and A. Dabas (2008), Dust emissions over the Sahel associated with the west African monsoon intertropical discontinuity region: A representative case-study, *Q. J. R. Meteorol. Soc.*, *134*(632), 621–634, doi:10.1002/qj.244.

Cakmur, R. V., R. L. Miller, and I. Tegen (2001), A comparison of seasonal and interannual variability of soil dust aerosols over the Atlantic Ocean as inferred by the TOMS AI and AVHRR AOT retrievals, *J. Geophys. Res.*, *106*(D16), 18,287–18,303, doi:10.1029/2000JD900525.

Carlson, T. N., and J. M. Prospero (1972), The large-scale movement of Saharan air outbreaks over the northern equatorial Atlantic, *J. Appl. Meteorol.*, *11*(2), 283–297, doi:10.1175/1520-0450(1972)011<0283:TLSMOS>2.0.CO;2.

Chiapello, I., G. Bergametti, L. Gomes, B. Chatenet, F. Dulac, J. Pimenta, and E. S. Suares (1995), An additional low layer transport of Sahelian and Saharan dust over the north–eastern tropical Atlantic, *Geophys. Res. Lett.*, *22*(23), 3191–3194, doi:10.1029/95GL03313.

Foltz, G. R., and M. J. McPhaden (2004), The 30–70 day oscillations in the tropical Atlantic, *Geophys. Res. Lett.*, *31*, L15205, doi:10.1029/2004GL020023.

Huang, J., C. Zhang, and J. M. Prospero (2010), African dust outbreaks: A satellite perspective of temporal and spatial variability over the tropical Atlantic Ocean, *J. Geophys. Res.*, *115*, D05202, doi:10.1029/2009JD012516.

Huffman, G. J., R. F. Adler, D. T. Bolvin, G. Gu, E. J. Nelkin, K. P. Bowman, Y. Hong, E. F. Stocker, and D. B. Wolff (2007), The TRMM multisatellite precipitation analysis (TMPA): Quasi-global, multiyear, combined-sensor precipitation estimates at fine scales, *J. Hydrometeorol.*, *8*(1), 38–55, doi:10.1175/JHM560.1.

Husar, R. B., J. M. Prospero, and L. L. Stowe (1997), Characterization of tropospheric aerosols over the oceans with the NOAA Advanced Very High Resolution Radiometer optical thickness operational product, *J. Geophys. Res.*, *102*(D14), 16,889–16,909, doi:10.1029/96JD04009.

Jones, C., N. Mahowald, and C. Luo (2004), Observational evidence of African desert dust intensification of easterly waves, *Geophys. Res. Lett.*, *31*, L17208, doi:10.1029/2004GL020107.

Karyampudi, V. M., et al. (1999), Validation of the Saharan dust plume conceptual model using lidar, Meteosat, and ECMWF data, *Bull. Am. Meteorol. Soc.*, *80*(6), 1045–1075, doi:10.1175/1520-0477(1999)080<1045:VOTSDP>2.0.CO;2.

Kaufman, Y. J., D. Tanre, L. A. Remer, E. F. Vermote, A. Chu, and B. N. Holben (1997), Operational remote sensing of tropospheric aerosol over land from EOS Moderate Resolution Imaging Spectroradiometer, *J. Geophys. Res.*, *102*(D14), 17,051–17,067, doi:10.1029/96JD03988.

Kaufman, Y. J., I. Koren, L. A. Remer, D. Tanré, P. Ginoux, and S. Fan (2005a), Dust transport and deposition observed from the Terra-Moderate Resolution Imaging Spectroradiometer (MODIS) spacecraft over the Atlantic Ocean, *J. Geophys. Res.*, *110*(D10), D10S12, doi:10.1029/2003JD004436.

Kaufman, Y. J., et al. (2005b), A critical examination of the residual cloud contamination and diurnal sampling effects on MODIS estimates of aerosol over ocean, *IEEE Trans. Geosci. Remote Sens.*, *43*(12), 2886–2897, doi:10.1109/TGRS.2005.858430.

Lau, W. K. M., and D. E. Waliser (Eds.) (2005), *Intraseasonal Variability of the Atmosphere-Ocean Climate System*, 474 pp., Springer, Heidelberg, Germany.

Leith, C. E. (1973), The standard error of time-average estimates of climatic means, *J. Appl. Meteorol.*, *12*(6), 1066–1069, doi:10.1175/1520-0450(1973)012<1066:TSEOTA>2.0.CO;2.

Levy, R. C., L. A. Remer, and O. Dubovik (2007a), Global aerosol optical properties and application to Moderate Resolution Imaging Spectroradiometer aerosol retrieval over land, *J. Geophys. Res.*, *112*(D13), D13210, doi:10.1029/2006JD007815.

Levy, R. C., L. A. Remer, S. Mattoo, E. F. Vermote, and Y. J. Kaufman (2007b), Second-generation operational algorithm: Retrieval of aerosol properties over land from inversion of Moderate Resolution Imaging Spectroradiometer spectral reflectance, *J. Geophys. Res.*, *112*, D13211, doi:10.1029/2006JD007811.

Levy, R. C., L. A. Remer, D. Tanré, S. Mattoo, and Y. J. Kaufman (2009), Algorithm for remote sensing of tropospheric aerosol over dark targets from MODIS: Collections 005 and 051: Revision 2, *MODIS Algorithm Theoretical Basis Document for the MOD04_L2 Product*, available at http://modis-atmos.gsfc.nasa.gov/_docs/ATBD_MOD04_C005_rev2.pdf.

Levy, R. C., L. A. Remer, R. G. Kleidman, S. Mattoo, C. Ichoku, R. Kahn, and T. F. Eck (2010), Global evaluation of the collection 5 MODIS dark-target aerosol products over land, *Atmos. Chem. Phys.*, *10*(21), 10,399–10,420, doi:10.5194/acp-10-10399-2010.

Li, K. F., B. Tian, D. E. Waliser, and Y. L. Yung (2010), Tropical mid-tropospheric CO2 variability driven by the Madden-Julian oscillation, *Proc. Natl. Acad. Sci. U. S. A.*, *107*(45), 19,171–19,175, doi:10.1073/pnas.1008222107.

Madden, R. A., and P. R. Julian (1971), Detection of a 40–50 day oscillation in the zonal wind in the tropical Pacific, *J. Atmos. Sci.*, *28*(5), 702–708, doi:10.1175/1520-0469(1971)028<0702:DOADOI>2.0.CO;2.

Madden, R. A., and P. R. Julian (1972), Description of global-scale circulation cells in the tropics with a 40–50 day period, *J. Atmos. Sci.*, *29*(6), 1109–1123, doi:10.1175/1520-0469(1972)029<1109:DOGSCC>2.0.CO;2.

Maloney, E. D., and J. Shaman (2008), Intraseasonal variability of the west African monsoon and Atlantic ITCZ, *J. Clim.*, *21*(12), 2898–2918, doi:10.1175/2007JCLI1999.1.

Matthews, A. J. (2004), Intraseasonal variability over tropical Africa during northern summer, *J. Clim.*, *17*(12), 2427–2440, doi:10.1175/1520-0442(2004)017<2427:IVOTAD>2.0.CO;2.

Prospero, J. M., and T. N. Carlson (1972), Vertical and areal distribution of Saharan dust over western equatorial north-Atlantic ocean, *J. Geophys. Res.*, *77*(27), 5255–5265, doi:10.1029/JC077i027p05255.

Prospero, J. M., and T. N. Carlson (1981), Saharan air outbreaks over the tropical North Atlantic, *Pure Appl. Geophys.*, *119*(3), 677–691, doi:10.1007/BF00878167.

Remer, L. A., et al. (2005), The MODIS aerosol algorithm, products, and validation, *J. Atmos. Sci.*, *62*(4), 947–973, doi:10.1175/JAS3385.1.

Remer, L. A., et al. (2008), Global aerosol climatology from the MODIS satellite sensors, *J. Geophys. Res.*, *113*, D14S07, doi:10.1029/2007JD009661.

Tanré, D., Y. J. Kaufman, M. Herman, and S. Mattoo (1997), Remote sensing of aerosol properties over oceans using the MODIS/EOS spectral radiances, *J. Geophys. Res.*, *102*(D14), 16,971–16,988, doi:10.1029/96JD03437.

Tian, B., Y. L. Yung, D. E. Waliser, T. Tyranowski, L. Kuai, E. J. Fetzer, and F. W. Irion (2007), Intraseasonal variations of the tropical total ozone and their connection to the Madden-Julian Oscillation, *Geophys. Res. Lett.*, *34*(8), L08704, doi:10.1029/2007GL029451.

Tian, B., et al. (2008), Does the Madden-Julian Oscillation influence aerosol variability?, *J. Geophys. Res.*, *113*, D12215, doi:10.1029/2007JD009372.

Tian, B., D. E. Waliser, E. J. Fetzer, and Y. L. Yung (2010), Vertical moist thermodynamic structure of the Madden-Julian Oscillation in Atmospheric Infrared Sounder retrievals: An update and a comparison to

ECMWF interim re-analysis, *Mon. Weather Rev.*, *138*(12), 4576–4582, doi:10.1175/2010MWR3486.1.

Waliser, D. E. (2005), Predictability and forecasting, in *Intraseasonal Variability in the Atmosphere–Ocean Climate System*, edited by W. K. M. Lau and D. E. Waliser, pp. 389–423, Springer, Berlin, doi:10.1007/3-540-27250-X_12.

Waliser, D., et al. (2009), MJO simulation diagnostics, *J. Clim.*, *22*(11), 3006–3030, doi:10.1175/2008JCLI2731.1.

Weare, B. C. (2010), Madden-Julian Oscillation in the tropical stratosphere, *J. Geophys. Res.*, *115*, D17113, doi:10.1029/2009JD013748.

Wheeler, M. C., and H. H. Hendon (2004), An all-season real-time multivariate MJO index: Development of an index for monitoring and prediction, *Mon. Weather Rev.*, *132*(8), 1917–1932, doi:10.1175/1520-0493(2004)132<1917:AARMMI>2.0.CO;2.

Wong, S., and A. E. Dessler (2007), Regulation of H_2O and CO in tropical tropopause layer by the Madden-Julian oscillation, *J. Geophys. Res.*, *112*, D14305, doi:10.1029/2006JD007940.

Wong, S., P. R. Colarco, and A. E. Dessler (2006), Principal component analysis of the evolution of the Saharan air layer and dust transport: Comparisons between a model simulation and MODIS and AIRS retrievals, *J. Geophys. Res.*, *111*, D20109, doi:10.1029/2006JD007093.

Zhang, C. (2005), Madden-Julian Oscillation, *Rev. Geophys.*, *43*, RG2003, doi:10.1029/2004RG000158.

R. A. Kahn, NASA Goddard Space Flight Center, 8800 Greenbelt Rd., Greenbelt, MD 20771, USA.

B. Tian, D. E. Waliser, and S. Wong, Jet Propulsion Laboratory, California Institute of Technology, M/S 183-501, 4800 Oak Grove Dr., Pasadena, CA 91109, USA. (baijun.tian@jpl.nasa.gov)